Appendix. Supplementary data

Multifunctional Gold Nanostar conjugates for Tumor Imaging and Combined Photothermal and Chemo-therapy

Haiyan Chen [a,†], Xin Zhang [a, †], Shuhang Dai[c], Yuxiang Ma [a], Sisi Cui [a], Samuel Achilefus[b,*], Yueqing Gu[a, *]

[a] *Department of Biomedical Engineering, State Key Laboratory of Natural Medicines and School of Life Science and Technology, China Pharmaceutical University, 24 Tongjia Lane, Gulou District, Nanjing 210009, China*

[b] *Department of Radiology, School of Medicine, Washington University, St. Louis , Missouri, United States*

[c] *Department of Pharmaceutical Science, School of Pharmacy, China Pharmaceutical University, 24 Tongjia Lane, Gulou District, Nanjing 210009, China*

[†] Haiyan Chen and Xin Zhang contributed equally to the work.

*Author to whom correspondence should be addressed:

Samuel Achilefu, PhD

Email: achilefus@mir.wustl.edu

Yueqing Gu, PhD

Email: guyueqing@cpu.edu.cn

Part 1: The mechanism illustration

For the conjugation of cRGD peptides and DOX with Au NS, we first attached GSH onto the surface of Au NS, GSH has both carboxyl and amino groups for further covalent conjugation. Subsequently, cRGD and DOX were immobilized onto Au NS via the covalent bonds with GSH to produce Au-cRGD, Au-DOX, and Au-cRGD-DOX. To track the targeted delivery of Au-RGD in vivo and verify its selective affinity to tumor sites, we also labeled Au-RGD with a hydrophilic indocyanine green (ICG) derivative, MPA to form a NIR fluorescent probe, Au-cRGD-MPA. Upon 765 nm NIR light irradiation, the NIR fluorescence (810 nm) emitted from Au-cRGD-MPA facilitated real time monitoring of the biodistribution of Au-cRGD, especially its tumor-targeting effectiveness in living subjects (Fiure S1A). Figure S1 illustrates the mechanisms of dual therapeutic effects by hyperthermia produced by Au NS upon NIR light irradiation and the anti-cancer drugs loaded on Au NS (Figure S1), the specific binding of Au-cRGD-MPA to integrin $\alpha_v\beta_3$ (Figure S1B)), and the positive tumor-targeting effect of Au-cRGD-DOX via integrin $\alpha_v\beta_3$ (Figure S1C)). Mechanistically, Au-cRGD-DOX first interacts with integrin $\alpha_v\beta_3$ located on the cell membrane, followed by the receptor mediated endocytosis. After releasing its ligand in the cytoplasm, the integrin $\alpha_v\beta_3$ recycles to the cell membrane.

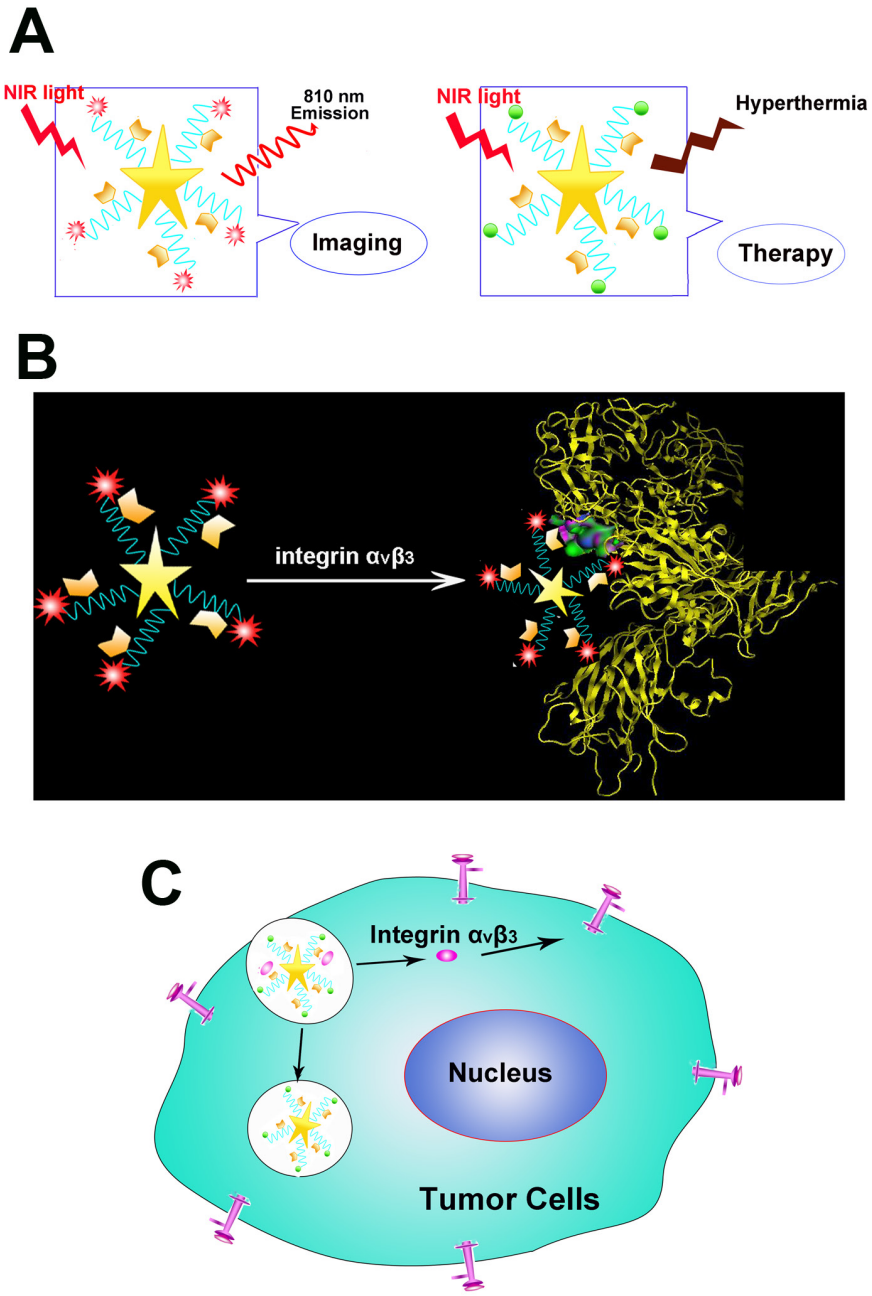

Figure S1: A) The dual therapeutic effects by hyperthermia produced by Au NS upon NIR light irradiation and the anti-cancer drugs loaded on Au NS; C) the specific binding of Au-cRGD-MPA to integrin $\alpha_v\beta_3$; B) the positive tumor-targeting effect of Au-cRGD-DOX via integrin $\alpha_v\beta_3$ on cell membrane.

Part 2: Synthesis routine and structures

For the conjugation of cRGD peptides and DOX with Au NS, we first attached GSH onto the surface of Au NS, GSH has both carboxyl and amino groups for further covalent conjugation. Subsequently, cRGD and DOX were immobilized onto Au NS via the covalent bonds with GSH to produce Au-cRGD, Au-DOX, and Au-cRGD-DOX. To track the targeted delivery of Au-RGD in vivo and verify its selective affinity to tumor sites, we also labeled Au-RGD with a hydrophilic indocyanine green (ICG) derivative, MPA to form a NIR fluorescent probe, Au-cRGD-MPA. The Synthesis routine and structures of Au-cRGD-DOX and Au-cRGD-MPA was shown in Figure S2.

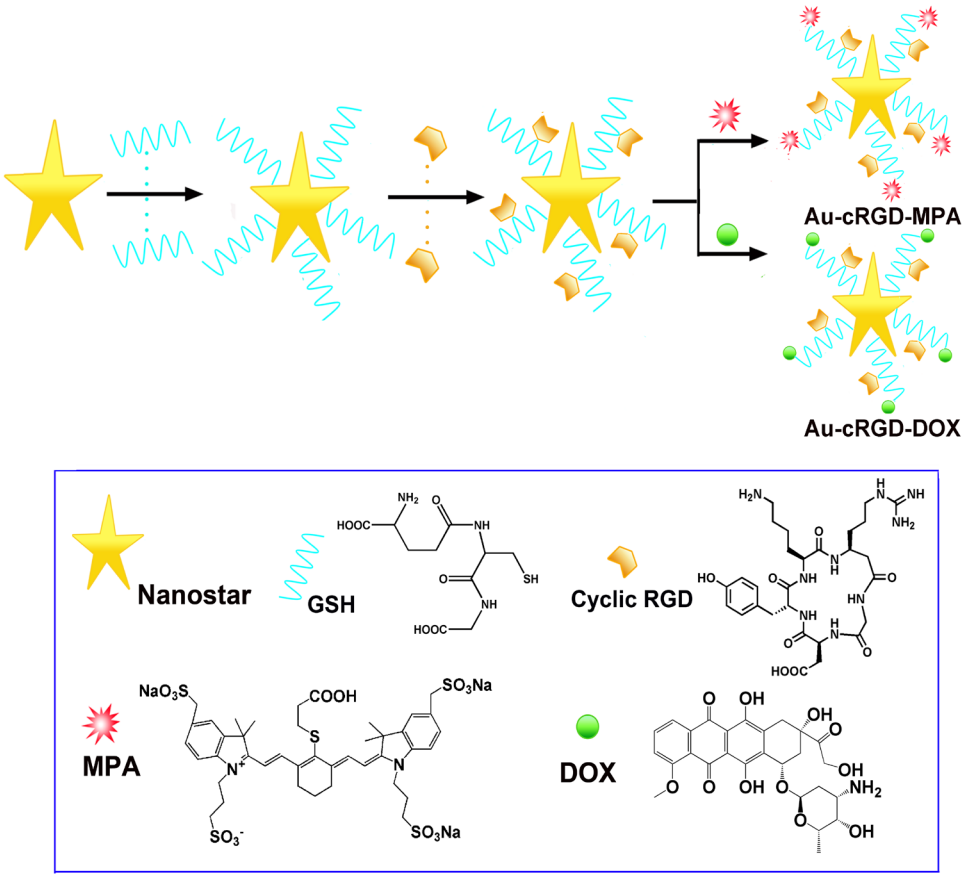

Figure S2: Synthesis routine and structures of Au-cRGD-DOX and Au-cRGD-MPA.

Part 3: FT-IR spectra

The Fourier transform infrared (FTIR) spectra of Au NS, Au-cRGD-MPA and Au-cRGD-DOX were recordedμ on a FTIR 8400S spectrometer (Shimadzu, Japan). As shown in Figure S3, the asymmetrical stretching vibration band at 1190.1 cm-1 and the symmetrical stretching vibration at 1034.9 cm-1 belong to S=O and the stretching vibration band at 637.0 cm^{-1} belongs to S-O, both attributable to the sulfoacid group of the capping agent, HEPES. The characteristic stretching and bending vibrations arising from the formation of amide bonds used to link Au NS with the conjugated ligands can be assigned as amide I: 1640.3 cm^{-1} (Figure S3B), 1638.1 cm^{-1} (Figure S3C) and amide II: 1563.1 cm^{-1}, 1560.1 cm^{-1} (Figure S3B). In addition, the bands 1184.0 cm^{-1} and 1045.0 cm^{-1} observed in the spectrum of Au-cRGD-MPA could be attributed to S=O stretching vibration of the sulfoacid group in MPA and could be used to differentiate Au-cRGD-MPA from Au-cRGD-DOX given that the characteristic sulfoacid band of Au NS disappeared after modification of DOX.

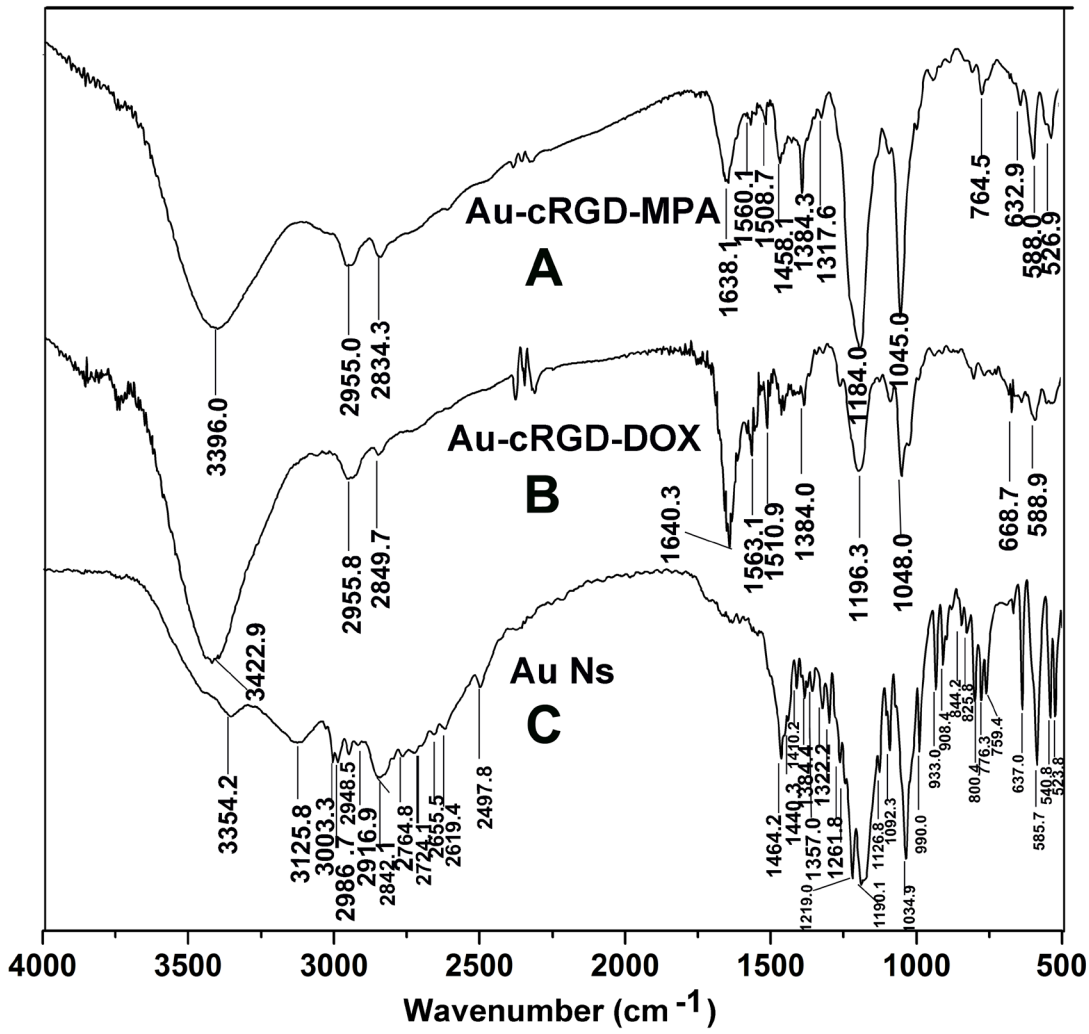

Figure S3: FT-IR spectroscopy of A) Au-cRGD-MPA, B) Au-cRGD-DOX and C) Au NS.

Part 4: Cytotoxicity evaluation of Au-cRGD-MPA

Cytotoxicity of Au NS, Au-MPA and Au-cRGD-MPA in different cell lines (MDA-MB-231, Bel7402 and MCF-7) was determined by MTT assay. The cells were seeded in 96-well plates (1×10^4 cells/well) and subsequently incubated for 24 h. After treating the cells with different concentrations (0.016 μg/mL to 10.0 μg/mL) of Au NS, Au-MPA and Au-cRGD-MPA, the cells were further maintained at 37 °C for 24 h.

Each well was replaced and the cells were washed three times with PBS (pH 7.0) before addition of 20 μL of MTT solution (5.0 μg/mL). After incubating another 4 h, the medium containing MTT was carefully removed from each well and DMSO (150 μL) was added to each well to dissolve the purple crystals. The plates were gently shaken for 10 min at room temperature before measuring the absorbance at 580 nm. All test samples were assayed in quadruplicate and the cell viability was calculated using the following formula: Cell viability = (Mean absorbance of test wells - Mean absorbance of medium control wells) / (Mean absorbance of untreated wells - Mean absorbance of medium control well) ×100%.

Determination of the cytotoxicity effects of Au-cRGD-MPA is a crucial criterion for its in vivo applicable. Therefore, we used MTT assay to determine this parameter in MDA-MB-231, Bel-7402 and MCF-7 cancer cells. The probe did not show significant cytotoxicity at concentrations up to 12.5 μM, with more than 80 % of the cells retaining viability after 24 h of treatment with 12.5 μM of Au NS, Au-MPA, or Au-cRGD-MPA (Figure S4). Interestingly, Au-cRGD-MPA maintained slightly higher cell viability than cells treated Au NS and Au-MPA. The observed low cytotoxicity could be attributed to several factors, including the non-toxic nature of the HEPES solution used in the particles formulation and the use of MPA, which is a derivative of indocyanine green (ICG) approved for human use. Moreover, the cell viability for some groups was larger than 100 %, which was impacted by the strong absorbance of Au NS. To further confirm the low toxicity of Au NS based nano-probes, the morphology of the cells including MDA-MB-231, Bel-7402 and

MCF-7 cancer cells after treating with Au NS based nanostructures was investigated by visual inspection using optical microscopy. The results indicated that no obvious morphology change was observed for these cell lines. These issues suggest that Au-cRGD-MPA could be a safe nanoprobe for clinical application.

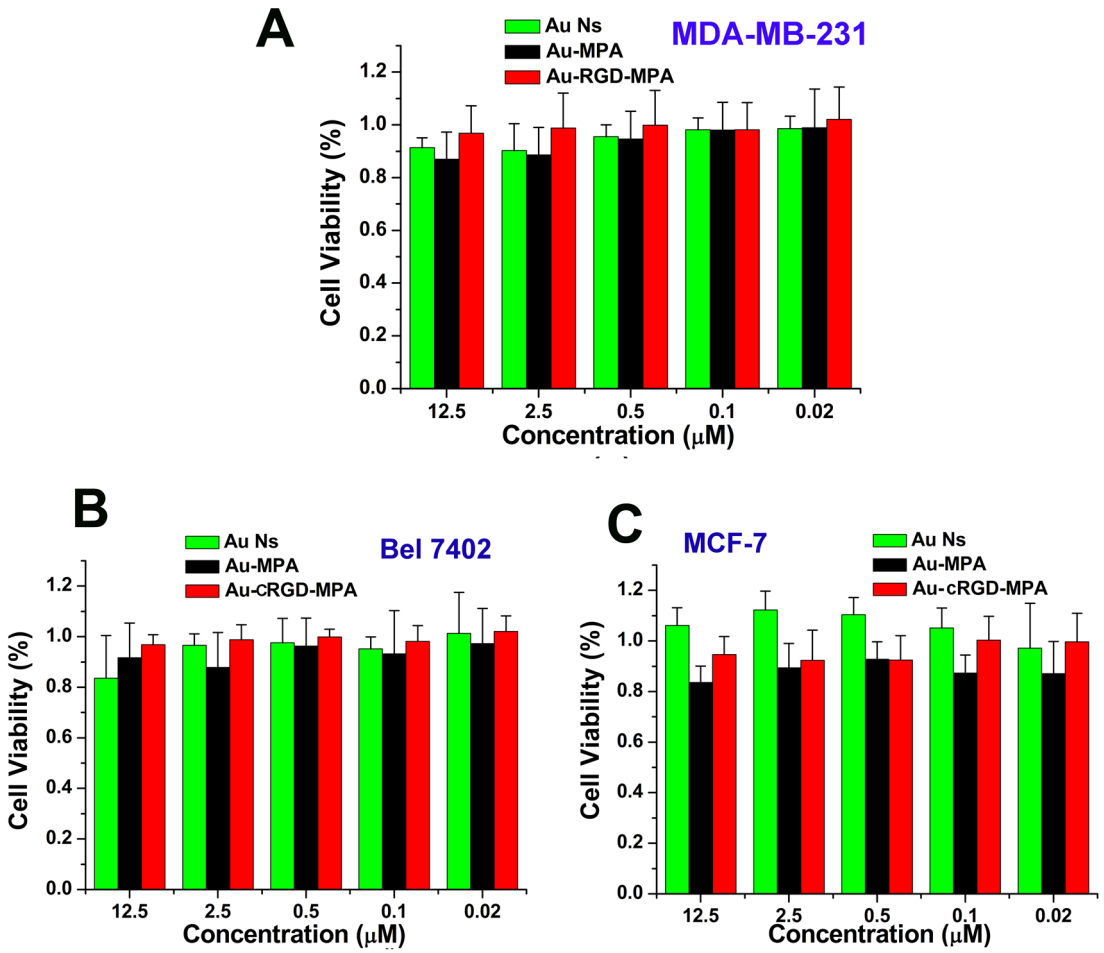

Figure S4: In vitro cytotoxicity studies of Au NS, Au-MPA, and Au-cRGD-MPA performed on A) MDA-MB-231, B) Bel-7402 and C) MCF-7 cell lines by MTT assays.

Part 5: Therapy evaluation of Au-cRGD-DOX in tumor-bearing mice

Tumors of the mice that received the photothermal and chemo-therapy from Au-cRGD-DOX via intratumoral or tail vein injection were obviously much smaller than those of other groups (Figure S5).

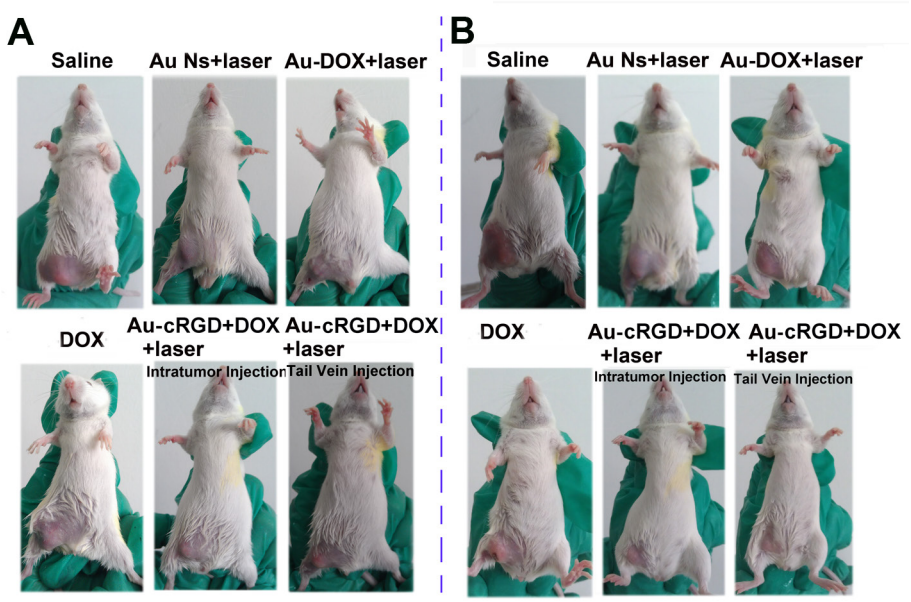

Figure S5: The pictures of tumor-bearing mice at A) 9 days and B) 18 days post-injection of saline, Au NS + light, Au-DOX + light, free DOX, Au-cRGD-DOX+ light (intratumoral injection) and Au-cRGD-DOX + light (tail vein injection) respectively.